An ultrasensitive and selective fluorescence nanosensor based on porphyrinic metal-organic framework (MOF) nanoparticles for Cu^{2+} detection in aqueous solution and living cells

Changming Cheng[1,2], Ruolin Zhang[1], Jiuhai Wang[1], Chunyi Wen[1], Youhua Tan[1], Mo Yang[1,3]*

[1]Department of Biomedical Engineering, the Hong Kong Polytechnic University, Hung Hom, Kowloon, Hong Kong SAR, PR China

[2]Institute of Nuclear Physics and Chemistry, China Academy of Engineering Physics (CAEP), Mianyang, PR China

[3]The Hong Kong Polytechnic University Shenzhen Research Institute, Shenzhen, PR China

Keywords:

ABSTRACT: Detecting trace amount of copper ions is of high importance since copper is an essential element in the environment and human body. Despite the recent advances in Cu^{2+} detection, the current approaches still suffer from insensitivity and lack of in-situ detection in living cells. In the present work, a fluorescence "turn-off" nanosensor based on porphyrinic metal-organic framework nanoparticles (MOF-525) is developed for sensitive and selective detection of Cu^{2+} in aqueous solutions and in living cells. The MOF-525 nanoparticles are prepared in a facile and environment-friendly hydrothermal route, which exhibit attractive properties including ultrasmall size, good water dispersity and intense red fluorescence. The fluorescence quenching of MOF-525 nanoparticles with high selectivity of Cu^{2+} is due to the strong binding of Cu^{2+} on porphyrin ligand through static quenching with a large Stern-Volmer quenching constant 2.56×10^7 M^{-1}. This MOF-525 nanoparticle based fluorescence sensor is used for Cu^{2+} detection in aqueous solution with a low limit of detection of 220 pM and a linear response range of 1.0~250 nM. Furthermore, this MOF-525 nanoparticle based fluorescence sensor has been successfully used for detection of intracellular Cu^{2+} in living cells with good cellular uptake due to small size and low cytotoxicity, which demonstrated its high potential for cellular sensing applications.

In chemical sensing and biosensing fields, Cu^{2+} is of great concern due to its important role in environmental and biological areas. It is one of common pollutants in the environment and excessive concentrations of copper in the body might cause damage to the liver and kidney.[1,2] Copper is one of essential metal elements in the human body and intracellular Cu^{2+} is important to some biological processes such as enzyme activities.[3] Both deficiency and excess of Cu^{2+} in human body would result in some diseases (e.g. Wilson disease, Alzheimer disease, Parkinson disease).[4] As such, it is highly desired to develop sensitive and selective sensing strategies for Cu^{2+} monitoring in environmental samples as well as in living cells.

The current detection techniques for metal ion detection include atomic absorption spectrometry,[5] inductively coupled plasma mass spectrometry (ICP-MS),[6] and inductively coupled plasma atomic emission spectrometry (ICP-AES).[7] However, they suffer from bulky instrumentation and complicated operation procedures. Various biosensing approaches have been developed for rapid and sensitive Cu^{2+} detection including electrochemical sensors,[8-10] colorimetric sensors.[11,12] However, these approaches are not suitable for intracellular Cu^{2+} detection in living cells. Fluorescence sensors have attracted a lot of attention for Cu^{2+} detection because they are relatively sensitive and simple set-up.[13,14] Fluorescence nanosensors based on various types of nanomaterials such as carbon dots,[15] quantum dots,[16] and gold nanoparticles[17] have been developed for Cu^{2+} detection in living cells. New fluorescence biosensors with high sensitivity, good photostability and specificity are always highly desirable for Cu^{2+} detection in living cells.

In the past few years, widespread attentions have been paid to a newly emerging family of porous materials with diverse structures as well as intriguing chemical and physical properties, metal-organic frameworks (MOFs). It is well known that MOFs are extended networks with interconnections of variable inorganic metal nodes and organic ligands, while they would inherit properties of both inorganic and organic moieties and exhibit great potential applications in the biomedical fields such as drug delivery,[18] bioimaging,[19] and sensing.[20] Pyrene-functionalized micro-sized MOF particles have been used for selective Cu^{2+} detection due to the selectively high affinity of Cu^{2+} to pyrene ligands.[21-22] However, these microporous MOF particles were not suitable for in-situ intracellular Cu^{2+} monitoring due to the difficulty for cellular uptake with large particle size and detection primarily in organic solutions. Furthermore, compared with bulk-phase or microscale sized MOFs, nanoporous MOFs (NMOFs) may exhibit distinguishing properties such as high surface area, abundant active sites and rapid response. Until now, there is no report about nanoporous MOFs based sensors for intracellular Cu^{2+} detection.

In this paper, we developed a fluorescence "turn-off" nanosensor based on porphyrinic metal-organic framework na-

noparticles (MOF-525) for sensitive detection of Cu^{2+} in aqueous solution and in living cells (Figure 1). Porphyrinic MOF nanoparticles (MOF-525) were synthesized with a hydrothermal route by using zirconium (IV) cluster and tetrakis(4-carboxyphenyl)porphyrin (TCPP) as metal node and organic ligand, respectively. Recently, low-cost and environment-friendly water has been used as the green solvent instead of classical organic solvents for the preparation of several MOFs including MFM-300(VIII),[23] Al-TCPP,[24] UiO-66-NH_2,[25] and HKUST-1.[26] However, to the best of our knowledge, there is few report on the water-based synthesis of nanostructured MOF-525 nanoparticles. The synthesized MOF-525 nanoparticles exhibited small size, intense red fluorescence emission and good water dispersity. In the presence of Cu^{2+}, the fluorescence signal of MOF-525 nanoparticles is quenched by Cu^{2+} selectively bound on the porphyrin TCPP ligand to form a non-fluorescent Cu-TCPP complex via electron transfer. This MOF-525 nanoparticle based fluorescence sensor was used for Cu^{2+} detection in aqueous solution with a low limit of detection (LOD) of 220 pM and a linear response range of 1.0~250 nM. Furthermore, this MOF-525 nanoparticle-based fluorescence sensor exhibited low cytotoxicity and was successfully used to detect intracellular Cu^{2+} in live Hela cells by monitoring changes of red fluorescent signal in living cells.

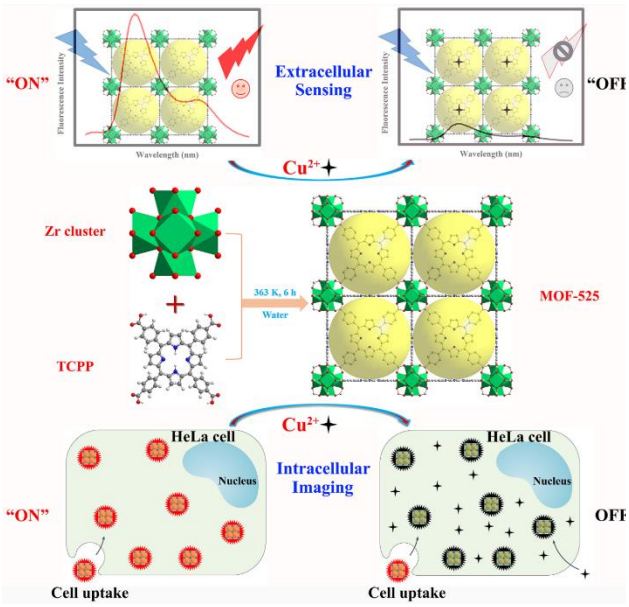

Figure 1. Schematic illustration of the preparation of porphyrinic MOF-525 nanoparticles and the "turn-off" fluorescence sensing mechanism for extracellular/intracellular detection of Cu^{2+}.

EXPERIMENTAL SECTION

Materials. Zirconium(IV) chloride ($ZrCl_4$, 98%), tetrakis(4-carboxylphenyl)-porphyrin (TCPP, 97 %), and Copper(II) nitrate trihydrate ($Cu(NO_3)_2{\cdot}3H_2O$, 99.99 %), were purchased from J&K Scientific Ltd. (Beijing, China). Acetic acid (HAc, 99.99 %), 3-(4,5-dimethylthiazol-2-yl)-2,5-diphenyltetrazolium bromide (MTT) and 4-(2-hydroxyethyl)-1-piperazineethanesulfonic acid (HEPES) buffer solution were purchased from Sigma (St. Louis, Mo, USA). Other chemicals were of analytical grade and used as received without any further purification.

Hydrothermal Preparation of MOF-525 Nanoparticles. MOF-525 nanoparticles were prepared according to previous work with some modification,[27] where water was used as the solvent instead of dimethylformamide. Typically, $ZrCl_4$ (0.01 mmol) and HAc (0.175 mmol) were firstly dissolved in 14.4 mL of deionized water, then followed by dropwise addition of TCPP (0.004 mmol) which was dissolved in 1.6 mL of NaOH solution (0.02 M). After stirring for 10 min, the resulting mixture solution was transferred into a 20 mL Teflon-lined stainless-steel autoclave and heated in an oven at 363 K for 6 h. After cooling down to room temperature naturally, the as-prepared sample was collected with centrifugation, washed with anhydrous ethanol and deionized water for several times to remove the possible unreacted precursors. Finally, the obtained product was re-dispersed in deionized water for further use.

Characterization. The powder XRD pattern was recorded with a Rigaku SmartLab diffractometer (Tokyo, Japan) using the Cu Kα source irradiation. TEM image was obtained with a JEOL Model JEM-2100F field emission electron microscopy (Tokyo, Japan). UV-vis absorption spectra were recorded on the Shimadzu UV-vis spectrophotometer (Kyoto, Japan). Fluorescence excitation/emission spectra and fluorescence decay curves were measured with an Edinburgh FLS920 photoluminescence spectrometer (Edinburgh, UK). Confocal fluorescence images were obtained with an Olympus FV1000-IX81 confocal laser scanning biological microscope (Tokyo, Japan) and a Leica TCS-SP5 confocal system (Heidelberg, Germany). MTT assay was conducted with a Tecan Infinite 200 microplate reader (TMaennedorf, Switzerland).

Fluorescence Sensing of Cu^{2+} in Aqueous Solutions. The fluorescence sensing of Cu^{2+} was carried out in HEPES buffer solution (20 mM, pH 7.4) in the presence of MOF-525 nanoparticles (5 mg L-1). After adding Cu^{2+} solution with different concentration into MOF-525 nanoparticle dispersion, fluorescence spectra in the wavelength range of 600 nm~750 nm under the excitation wavelength of 414 nm were recorded. For selectivity experiments, metal ions (i.e. Mg^{2+}, Zn^{2+}, Ca^{2+}, Cd^{2+}, Fe^{2+}, Fe^{3+}, Co^{2+}, Ni^{2+} and Cu^{2+}) with the concentration of 250 nM were added into MOF-525 nanoparticle dispersion, and the quenching effect of different metal ion on the fluorescence of MOF-525 nanoparticle solution was investigated.

Cell Viability of MOF-525 Nanoparticles. MTT assay was conducted to evaluate the cytotoxicity of MOF-525 nanoparticles to HeLa cells. Firstly, HeLa cells were seeded in a 96-well plate at a density of 1.0×104 well-1 and cultured in Dulbecco's modified Eagle medium in the presence of 10 % fetal bovine serum and 1 % penicillin/streptomycin in an incubator (37°C, 5 % CO_2) for 24 h. Then, MOF-525 nanoparticles with different concentration (10~60 mg L-1) was added into the well (100 μL $well^{-1}$) and cultured for 24 h. After discarding the solution, 100 μL cell medium containing MTT (10 μL, 5 g L^{-1}) was added into each well, and further incubated for 4 h. Then, 100 μL dimethyl sulfoxide was added into each well to replace the cell medium, and another 10 min incubation was performed. The control group was performed with the same procedure in the absence of MOF-525 nanoparticles. Finally, absorbance value at the wavelength of 490 nm in each well was recorded and the cell viability was calculated with the following formula:

$$\text{Cell viability}\ (\%) = (A_s - A_b)/(A_c - A_b) \times 100\ \% \quad (1)$$

where A_s, A_b, A_c were absorbance values of experimental group, blank well and control group, respectively.

Intracellular Cu^{2+} detection. Prior to intracellular Cu^{2+} imaging, HeLa cells were cultured in petri dishes at a density of 1.0×10^6 well^{-1} and treated with 30 mg L^{-1} MOF-525 nanoparticles for incubation of 1 h at 37 °C (5 % CO_2). After incubation, Hela cells were washed with PBS for three times. Then, exogenous Cu^{2+} solution with a final concentration of 50 nM was added and incubated with HeLa cells for another 1 h. The control cell group was treated with the same procedure in the absence of MOF-525 nanoparticles. After washing with PBS for three times, confocal fluorescence images of HeLa cells were taken at emission 550~800 nm range under the excitation wavelength of 405 nm.

RESULTS AND DISCUSSIONS

Synthesis and Characterization of MOF-525 Nanoparticles. In the present work, a facile and environment-friendly hydrothermal route was successfully employed for the preparation of ultrasmall fluorescent MOF-525 nanoparticles for the first time. The morphology and size of as-prepared sample were firstly characterized with TEM (Figure 2a). It could be observed clearly that the sample were nearly spherical crystals with the average size of 5 nm, as revealed in the insets of Figure 2a. The ultrasmall size of as-prepared sample could be attributed to the low concentration of precursors and relatively mild reaction condition. It is worth pointing out that the cubic crystal with regular shape and sharp edge of typical MOF-525 was not observed in the present work probably due to the ultrasmall size. The similar phenomena have been reported in the previous works.[28-30]

Powder XRD measurement was then exploited to identify the crystalline phase of as-prepared sample. Figure 2b displayed the typical XRD pattern of the sample prepared in the present work and simulated XRD pattern of MOF-525.[27] As shown in Figure 2b (pattern i), the simulated XRD pattern of MOF-525 exhibited a prominent diffraction peak at 4.5° as well as other diffraction peaks at 6.4°, 7.8°, and 9.1°. A distinct diffraction peak centered at 4.5° along with a shoulder peak covering diffraction peaks at 6.4° and 7.8° could be observed on as-prepared sample (Figure 2b, pattern ii), which was consistent with simulated XRD pattern of MOF-525 (Figure 2b, pattern i). The diffraction peak centered at 9.1° was unconspicuous on the XRD pattern of as-prepared sample, which might be attributed to the ultrasmall size. The similar phenomena have been reported in previous works.[31,32] The broad diffraction peaks of the as-prepared sample were consistent with the ultrasmall size characteristic as depicted in Figure 2a. The aforementioned results demonstrated that ultrasmall MOF-525 NCs were successfully prepared with a hydrothermal approach by using water as the green solvent instead of dimethylformamide, which was widely employed in the previous work for the preparation of MOF-525.[27]

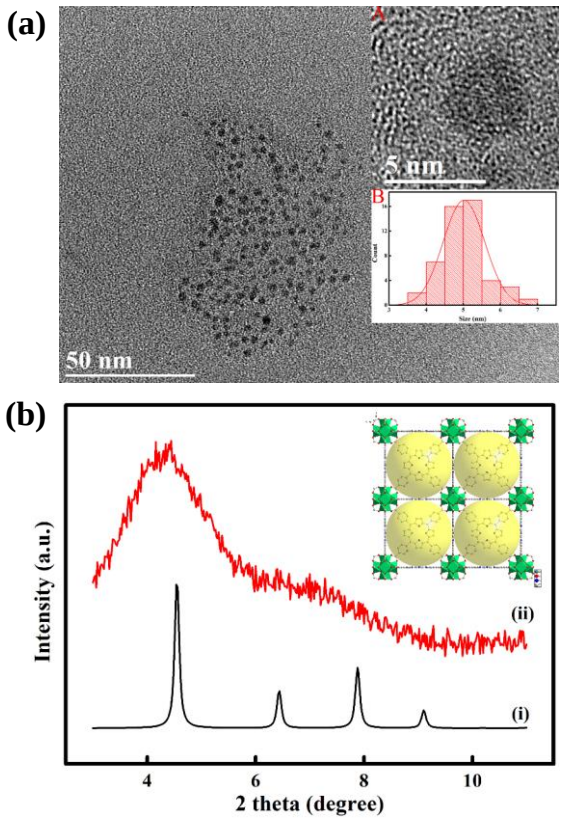

Figure 2. (a) TEM image of as-prepared MOF-525 nanoparticles, insets: A: spherical single MOF-525 nanoparticle; B: size distribution; (b) XRD patterns of (i) simulated MOF-525 and (ii) as-prepared MOF-525 nanoparticles, inset: crystal structure of MOF-525.

The optical properties of MOF-525 nanoparticles in the HEPES solution (20 mM, pH=7.4) were investigated, as depicted in Figure 3a. The UV-Vis absorption spectrum of MOF-525 nanoparticles exhibited a Soret band at 414 nm (curve a). It was observed that the fluorescence excitation spectrum of MOF-525 nanoparticles was similar to UV-Vis absorption spectrum (curve b). Under excitation at 414 nm, MOF-525 nanoparticles would display a strong emission peak at 646 nm and a shoulder peak centered at 704 nm, respectively (curve c). The inset of Figure 3a depicted the photographs of MOF-525 nanoparticles dispersed in HEPES solution under (left) visible light and (right) UV light. It could be clearly observed that MOF-525 nanoparticles were dispersed well in the aqueous medium without apparent aggregation, which could be attributed to the ultrasmall size of MOF-525 nanoparticles. In addition, the zeta-potential of MOF-525 nanoparticles was measured to be ~-30 mV, confirming again their good water dispersity (Figure S1). The characteristic red fluorescence of MOF-525 nanoparticles was strong enough to be observed easily by naked eye under the UV light excitation (inset of Figure 3a). Inspired by the intense fluorescence as well as excellent water dispersity, it is anticipated that MOF-525 nanoparticles would be potentially exploited as efficient fluorescence probe in the sensing field. For this purpose, as one of major concerns in fluorescence sensors, the fluorescence stability of

MOF-525 nanoparticles was investigated by monitoring the change of fluorescence intensity at 646 nm under successive light excitation at 414 nm. As shown in Figure 3b, no obvious photobleaching behavior was observed and the fluorescence signal was quite stable with a relative standard deviation (RSD) of 0.32 %, which validated the feasibility of MOF-525 nanoparticles as fluorescence probe for sensor construction.

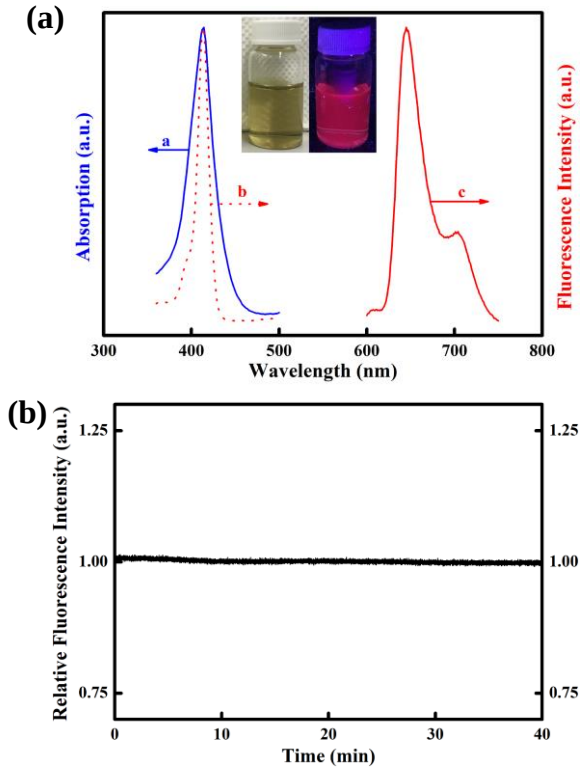

Figure 3. (a) UV-Vis absorption, excitation and emission spectra of MOF-525 nanoparticles, inset: photographs of MOF-525 nanoparticles under (left) visible and (right) UV light; (b) fluorescence stability testing of MOF-525 nanoparticles.

Fluorescence Sensing of Cu^{2+} in Aqueous Solutions. Due to the good water dispersity, the synthesized MOF-525 nanoparticle could be used for detection of Cu^{2+} in aqueous solutions. Fluorescence spectra of MOF-525 nanoparticle solution in the presence of Cu^{2+} with different concentrations were recorded. As shown in Figure 4a, it could be clearly observed that the fluorescence intensity decreased progressively with the increase of Cu^{2+} concentration. F_0/F was used as an indicator to show the fluorescence signal change due to Cu^{2+} quenching, where F_0 and F were fluorescence intensities at 646 nm in the absence and presence of Cu^{2+}, respectively. The correlation between F_0/F and Cu^{2+} concentration in solution was shown in Figure 4b. A linear correlation between F_0/F and Cu^{2+} concentration from 1.0 nM to 250 nM was observed with a correlation coefficient of 0.9981. The limit of detection (LOD) was calculated to be as low as 220 pM, which was calculated as control signal plus 3 times of standard derivation. Furthermore, the Stern-Volmer (SV) equation is expressed as the equation (1):

$$F_0/F = K_{sv}[Q] + 1 \qquad (1)$$

where F_0, F, K_{sv} and $[Q]$ represented fluorescence intensity of MOF-525 nanoparticle dispersion in the absence of Cu^{2+}, fluorescence intensity of MOF-525 nanoparticles dispersion in the presence of Cu^{2+}, Stern-Volmer quenching constant and molar concentration of Cu^{2+}, respectively. According to the equation (1), the Stern-Volmer quenching constant (K_{sv}) was estimated to be 2.56×107 M^{-1}, indicating the excellent quenching ability of Cu^{2+} on the fluorescence of MOF-525 nanoparticles. The aforementioned results demonstrated that this MOF-525 nanoparticle based nanosensor for Cu^{2+} detection high quenching constant and low LOD of 220 pM, which was somewhat better or comparable with other nanomaterials based fluorescence sensors for Cu^{2+} detection as shown in Table 1.[33-40] Herein, the potential application of MOF nanoparticles in the sensing field was expanded and an alternative sensing strategy towards Cu^{2+} was developed. More importantly, the MOF-525 nanoparticle based fluorescence sensor for detection of Cu^{2+} could work in the totally aqueous medium, indicating its promising potential in the biological research field.

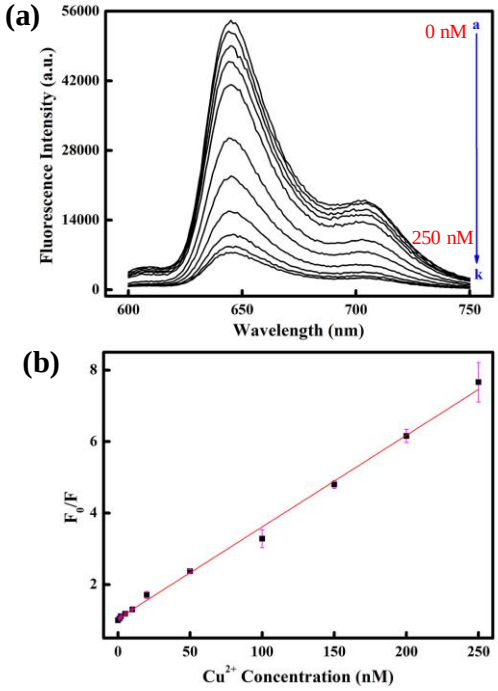

Figure 4. (a) Fluorescence spectra of MOF-525 NCs (5 mg L^{-1}) in HEPES buffer solution (20 mM, pH 7.4) under the excitation at 414 nm in the presence of Cu^{2+} with different concentration (a~k: 0~250 nM); (b) Plot of F_0/F against the concentration of Cu^{2+}, where the F_0 and F were the fluorescence intensities at 646 nm in the absence and presence of Cu^{2+}, respectively.

Sensing Mechanism and Specificity of Cu^{2+} Detection. The possible quenching mechanism between MOF-525 nanoparticles and Cu^{2+} and the specificity of Cu^{2+} sensing were then explored. Generally, fluorescence quenching processes can be divided into two types: static quenching and dynamic quenching. Considering the large Stern-Volmer quenching constant (2.56×10^7 M^{-1}), it was speculated that the fluorescence of MOF-525 nanoparticles might be statically quenched

by Cu^{2+} in this work. According to the static quenching mechanism, the fluorescence lifetime of fluorophore would not be affected by quencher along with the formation of nonfluorescent complex between fluorophore and quencher. Firstly, time-resolved fluorescence lifetime experiment was performed. The fluorescence decay curves of MOF in the absence and presence of Cu^{2+} were measured under 414 nm laser pulse excitation (Figure 5a). Fluorescence lifetime values of MOF-525 nanoparticles in the absence and presence of Cu^{2+} were calculated to be 9.93 ns and 9.92 ns, respectively. The similar decay curves and fluorescence lifetime revealed that the quenching process was predominantly static quenching. Considering the crystal structure of MOF-525 as depicted in the inset of Fig. 2b, the free-base porphyrin center in MOF-525 nanoparticles would be metalated with Cu^{2+} along with the formation of nonfluorescent complex due to the strong binding force between Cu^{2+} and pyrene group. Secondly, it was observed that the UV-Vis absorption spectrum of MOF-525 nanoparticle solution would have a blue shift after the addition of Cu^{2+} (Figure 5b). This blue shift of UV-Vis absorption spectrum is due to the formation of MOF-525-Cu^{2+} complex, which was also observed during the binding of Cu^{2+} with other porphyrinic ligands.[41] As such, it could be concluded that the fluorescence of MOF-525 nanoparticles was statically quenched with Cu^{2+}.

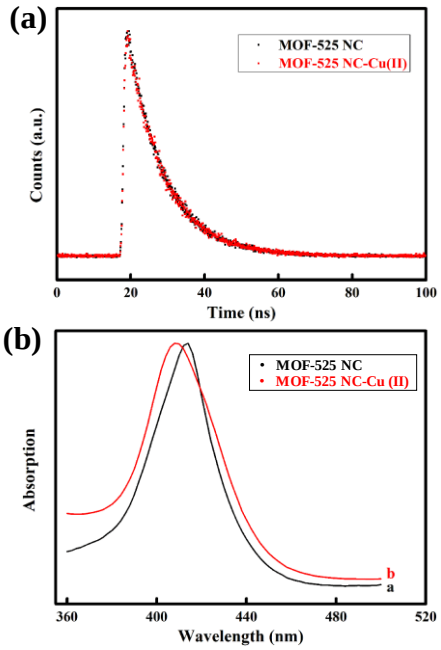

Figure 5. (a) The time-resolved fluorescence decay curves and (b) UV-Vis absorption spectra of MOF-525 nanoparticle dispersion in the absence and presence of Cu^{2+}.

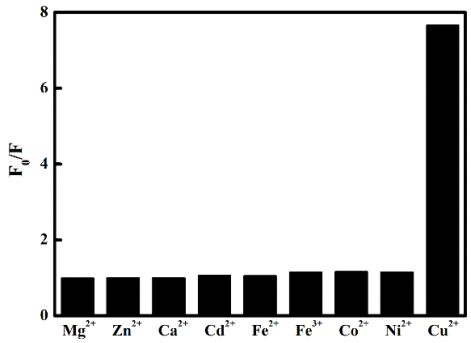

Figure 6. The average value of F0/F for various metal ions (i.e. Mg^{2+}, Zn^{2+}, Ca^{2+}, Cd^{2+}, Fe^{2+}, Fe^{3+}, Co^{2+}, Ni^{2+} and Cu^{2+}) at a concentration of 250 nM for quenching effect comparison of MOF-525 nanoparticles (n=5).

Not only sensitivity, but also selectivity was of great importance for the proposed fluorescence sensor. Quenching effects of various metal ions (i.e. Mg^{2+}, Zn^{2+}, Ca^{2+}, Cd^{2+}, Fe^{2+}, Fe^{3+}, Co^{2+}, Ni^{2+} and

Table 1. Comparison of different fluorescent sensors for Cu^{2+} detection.

Fluorescence probe	Linear range (nM)	Limit of detection (nM)	Reference
[a]g-C_3N_4 NSs	0~45	1.2	(Cheng et al. 2014)
[b]P,O-g-C_3N_4 NDs	0~1000	2	(Rong et al. 2015)
[c]BPEI-CQDs	10~1100	6	(Dong et al. 2012)
[d]CdSe/ZnS QDs	0~600	0.15	(Jin and Han 2014)
[e]SiO_2@ZIF-8 NPs	10~500	3.8	(Song et al. 2015)
[f]Au-Ag NCs	0.5~2500	0.30	(Zhang et al. 2014)
[g]PEI-Ag NCs	10~7700	10	(Yuan et al. 2014)
[h]CdTe QDs	10~1000	2.3	(Zhao et al. 2013)
[i]MOF-525 NCs	1.0~250	0.22	This work

[a]g-C_3N_4 NSs: graphitic carbon nitride nanosheets;
[b]P,O-g-C_3N_4 NDs: phosphorus, oxygen-doped graphitic carbon nitride nanodots;
[c]BPEI-CQDs: poly(ethylenimine)-functionalized carbon quantum dots;
[d]CdSe/ZnS QDs: CdSe/ZnS quantum dots;
[e]SiO_2@ZIF-8 NPs: SiO_2@zeolitic imidazolate framework-8 nanoparticles;
[f]Au-Ag NCs: gold-silver nanoclusters;
[g]PEI-Ag NCs: polyethyleneimine-protected silver nanoclusters;
[h]CdTe QDs: CdTe quantum dots;
[i]MOF-525 NCs: metal-organic framework-525 nanocrystals;

Cu^{2+}) at a concentration of 250 nM on the fluorescence intensity of MOF-525 nanoparticles were explored. F_0/F was used as an indicator to show the fluorescence signal change due to Cu^{2+} quenching, where F_0 and F were fluorescence intensities at 646 nm in the absence and presence of Cu^{2+}, respectively. The average value of F_0/F (n=5) was used for comparison. As shown in Figure 6, there is no obvious quenching effects of Mg^{2+}, Zn^{2+}, Ca^{2+}, Cd^{2+}, Fe^{2+}, Fe^{3+}, Co^{2+} and Ni^{2+} on fluorescence intensity of MOF-525 nanoparticles compared with Cu^{2+}, revealing that the proposed fluorescent MOF-525 nanosensor had excellent selectivity for Cu2+ over other kinds of common metal ions. The great selectivity of the proposed fluorescent nanosensor could be attributed to the much higher binding affinity of Cu^{2+} to nitrogen atoms in the porphyrin centers in MOF-525 nanoparticles compared to other metal ions. The selective higher binding force between Cu^{2+} and porphyrin ligands have been reported in the previous research work.[21,22]

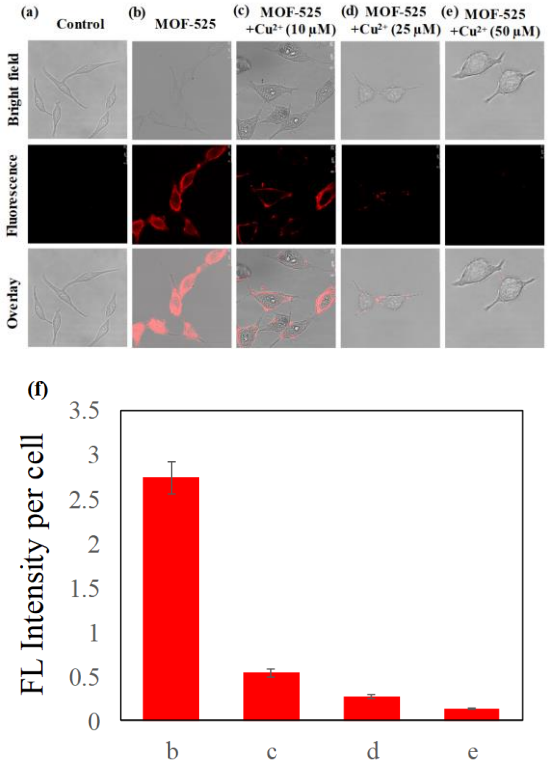

Figure 7. Confocal fluorescence images of HeLa cells in the presence of (a) no treatment; (b) MOF-525 nanoparticles (30 mg L-1); (c) MOF-525 nanoparticles & 10 μM Cu^{2+}; (d) MOF-525 nanoparticles & 25 μM Cu^{2+}; (e) MOF-525 nanoparticles & 50 μM Cu^{2+}. Scale bar: 25 μm.

Intercellular Sensing of Cu^{2+} in Living Cells. Owing to unique advantages of as-prepared MOF-525 nanoparticles including ultrasmall size, good water dispersity, good photostability and intense fluorescence, it was anticipated MOF-525 nanoparticle based nanosensor could be an excellent candidate for intracellular Cu^{2+} detection. In order to confirm this possibility, the cytotoxicity of MOF-525 nanoparticles was firstly investigated by MTT assays for HeLa cells incubated with various concentrations of MOF-525 nanoparticles (Figure S2). No obvious cytotoxicity against HeLa cells was observed after 24 h with viability over 80 % at the concentrations below 30 mg L^{-1}, demonstrating the acceptable biocompatibility, low cytotoxicity as well as great potential in cell imaging. Then, the potential application of MOF-525 nanoparticles for intracellular monitoring of Cu^{2+} was studied in living HeLa cells. As shown in Figure 7a, HeLa cells without incubation with MOF-525 nanoparticles did not shown obvious red fluorescence under the excitation wavelength of 405 nm. Significant red fluorescence could be observed in HeLa cells after incubation with MOF-525 nanoparticles with concentration of 30 mg L^{-1} (Figure 7b, 7f). These results confirmed the penetration of MOF-525 nanoparticles into the living cells and the potential of our assay in sensing intracellular Cu^{2+}. MOF-525 labelled Hela cells were then incubated with different exogenous concentrations of Cu^{2+} (10 μM, 25 μM and 50 μM) for 30 min. The quantified mean fluorescence intensity per cell for various Cu^{2+} concentrations was analyzed using Image J software. Fluorescent image signals of Hela cells gradually became weaker with a Cu^{2+} concentration-dependent manner until completely quenching (Figure 7c, 7d, 7e and 7f). These results demonstrated the capability of the nanosensor in Cu^{2+} imaging and detection of living cells.

CONCLUSION

In the present work, porphyrinic MOF nanoparticles (MOF-525) based fluorescent nanobiosensor was successfully developed for Cu^{2+} sensing in aqueous solutions with a wide linear range (1.0~250 nM), low limit of detection (220 pM) and high quenching constant (2.56×10^7 M^{-1}). Furthermore, this MOF-525 nanoparticle based fluorescence sensor has been successfully used for detection of Cu^{2+} in living Hela cells with good cellular uptake due to small size, excellent photostability and low cytotoxicity. The present research would offer an alternative fluorescence sensing and intracellular imaging strategy for Cu^{2+}, and expend the potential application of MOFs in the fields of sensing and bioimaging.

ASSOCIATED CONTENT

Supporting Information

The Supporting Information is available free of charge on the ACS Publications website.

Zeta-potential results, and MTT assay results (PDF)

AUTHOR INFORMATION

Corresponding Author

* E_mail: Mo.Yang@polyu.edu.hk

ORCID

Mo Yang: 0000-0002-3863-8187

†If an author's address is different than the one given in the affiliation line, this information may be included here.

Notes

The authors declare no competing financial interest.

ACKNOWLEDGMENT

This work was supported by the National Natural Science Foundation of China (NSFC) (Grant No. 31771077), and The Hong Kong Polytechnic University Internal Fund (1-ZVJ7 and 1-YW1L). This work was also supported by the University Research Facility in Life Sciences of the Hong Kong Polytechnic University.

ABBREVIATIONS

MOF	metal-organic framework (MOF)
XRD	X-ray diffraction
TEM	transmission electron microscope

REFERENCES

(1) Barranguet, C.; van den Ende, F. P.; Rutgers, M.; Breure, A M.; Greijdanus, M.; Sinke, J.J.; Admiraal, W. *Environ. Toxicol. Chem.* **2003,** *22*, 1340−1349.

(2) Hu, R.; Furukawa, T.; Wang, X.; Nagatsu, M. *Adv. Funct. Mater*. **2017**, *27*, 1702232.

(3) Zhu, A.; Qu, Q.; Shao, X.; Kong, B.; Tian, Y. *Angew. Chem. Int. Ed.* **2012**, *51*, 7185-7189.

(4) Bandmann O.; Weiss, K.H.; Kaler, S.G. *Lancet Neurol.*, **2015**, *14*, 103-113.

(5) Lima, G.F.; Ohara, M.O.; Clausen, D.N.; Nascimento, D.R.; Ribeiro, E.S.; Segatelli, M.G.; Bezerra, M.A.; Tarley, C.R.T. *Microchim. Acta* **2012**, *178*, 61-70.

(6) Li, Y.; Chen, C.; Li, B.; Sun, J.; Wang, J.; Gao, Y.; Zhao, Y.; Chai, Z.J. *J. Anal. At. Spectrom.* **2006**, *21*, 94- 96.

(7) Liu, Y.; Liang, P.; Guo, L. *Talanta*, **2005**, *68*, 25-30.

(8) Cheng, C.; Huang, Y.; Tian, X.; Zheng, B.; Li, Y.; Yuan, H.; Xiao, D.; Xie, S.; Choi, M.M.F. *Anal. Chem.* **2012**, *84*, 4754-4759

(9) Zhang, J.; Cheng, C.; Huang, Y.; Qian, L.; Zheng, B.; Yuan, H.; Guo, Y.; Xiao, D. *Analyst* **2013**, *138*, 2073-2079.

(10) Li, J.P.; Zhang, L.M.; Wei, G.; Zhang, Y.; Zeng, Y. *Biosen. Bioelectron.* **2015**, *69*, 316-320.

(11) Shen, Q.P.; Li, W.H.; Tang, S.Y.; Hu, Y.F.; Nie, Z.; Huang, Y.; Yao, S.Z. *Biosens. Bioelectron.* **2013**, *41*, 663-668.

(12) Yin, K.; Li, B.W.; Wang, X.C.; Zhang, W.W.; Chen, L.X. *Biosen. Bioelectron.* **2015**, *64*, 81-87.

(13) Hao, Y.Q., Liu, L., Long, Y.F., Wang, J.X., Liu, Y.N., Zhou, F.M., *Biosen. Bioelectron*. **2013**, *41*, 723-729.

(14) Zhang, H.T., Feng, L., Jiang, Y., Wong, Y.T., He, Y.H., Zheng, G.S., He, J., Tan, Y., Sun, H.Y., Ho, D., 2017. *Biosens. Bioelectron.* 94, 24-29.

(15) Lu, L.L., Feng, C.C., Xu, J., Wang, F.Y., Yu, H.J., Xu, Z.A., Zhang, W., 2017a. Biosens. Bioelectron. 92, 101-108.

(16) Zou, C., Foda, M.F., Tan, X., Shao, K., Wu, L., Lu, Z., Bahlol, H.S., Han, H., 2016. Anal. Chem. 88, 7395-7403.

(17) Li, L., Feng, J., Fan, Y., Tang, B., 2015b. Anal. Chem. 87, 4829-4835.

(18)Wu, M.X., Yang, Y.W., 2017. Adv. Mater. 29, 1606134.

(19) Du, T., Zhao, C., ur Rehman, F., Lai, L.M., Li, X., Sun, Y., Luo, S., Jiang, H., Gu, N., Selke, M., Wang, X., 2017. Adv. Funct. Mater. 27, 1603926.

(20) Kreno, L.E., Leong, K., Farha, O.K., Allendorf, M., Van Duyne, R.P., Hupp, J.T., 2012. Chemical Reviews 112, 1105-1125.

(21)Xiao, Y., Cui, Y., Zheng, Q., Xiang, S., Qian, G., Chen, B., 2010, Chem. Commun. 46, 5503–5505.

(22) Cho, W., Lee, H. J.. Choi, G., Choi, S., Oh, M., 2014. J. Am. Chem. Soc. 136, 12201–12204 .

(23) Lu, Z., Godfrey, H.G.W., da Silva, I., Cheng, Y., Savage, M., Tuna, F., McInnes, E.J.L., Teat, S.J., Gagnon, K.J., Frogley, M.D., Manuel, P., Rudić, S., Ramirez-Cuesta, A.J., Easun, T.L., Yang, S., Schröder, M., 2017b. Nat. Commun. 8, 14212.

(24) Fang, X., Shang, Q., Wang, Y., Jiao, L., Yao, T., Li, Y., Zhang, Q., Luo, Y., Jiang, H.-L., 2018. Adv. Mater. 30, 1705112.

(25) Li, K., Lin, S., Li, Y., Zhuang, Q., Gu, J., 2018b. Angew. Chem. Int. Ed. 57(13), 3439-3443.

(26) Röder, R., Preiß, T., Hirschle, P., Steinborn, B., Zimpel, A., Höhn, M., Rädler, J.O., Bein, T., Wagner, E., Wuttke, S., Lächelt, U., 2017. J. Am. Chem. Soc. 139, 2359-2368.

(27) Morris, W.; Volosskiy, B., Demir, S., Gándara, F., McGrier, P.L., Furukawa, H., Cascio, D., Stoddart, J.F., Yaghi, O.M., 2012. Inorg. Chem. 51, 6443-6445.

(28) Park, J., Jiang, Q., Feng, D.W., Mao, L.Q., Zhou, H.C., 2016. J. Am. Chem. Soc. 138(10), 3518-3525.

(29) Zhuang, J., Kuo, C.H., Chou, L.Y., Liu, D.Y., Weerapana, E., Tsung, C.K., 2014. ACS Nano 8, 2812-2819.

(30) Kung, C., Li, Y., Lee, M., Wang, S., Chiang, W., Ho, K., 2016. J. Mater. Chem. A 4, 10673-10682.

(31)Wu, Q., Zhou, M., Shi, J., Li, Q.J., Yang, M.Y., Zhang, Z.X., 2017. Anal. Chem. 89, 6616-6623.

(32) Ryu, U., Jee, S., Park, J.-S., Han, I.K., Lee, J.H., Park, M., Choi, K.M., 2018. ACS Nano 12(5), 4968-4975.

(33) Cheng, N.Y., Jiang, P., Liu, Q., Tian, J.Q., Asiri, A.M., Sun, X.P., 2014. Analyst 139, 5065-5068.

(34) Rong, M.C., Song, X.H., Zhao, T.T., Yao, Q.H., Wang, Y.R., Chen, X., 2015. J. Mater. Chem. C 3, 10916-10924.

(35) Dong, Y.Q., Wang, R.X., Li, G., Chen, C.Q., Chi, Y.W., Chen, G.N., 2012. Anal. Chem. 84, 6220-6224.

(36) Jin, L.H., Han, C.S., 2014. Anal. Chem. 86, 7209-7213.

(37) Song, Y., Hu, D., Liu, F., Chen, S., Wang, L., 2015. Analyst 140, 623-629.

(38) Zhang, N., Si, Y.M., Sun, Z.Z., Chen, L.J., Li, R., Qiao, Y.C., Wang, H., 2014. Anal. Chem. 86(23), 11714-11721.

(39) Yuan, Z.Q., Cai, N., Du, Y., He, Y., Yeung, E.S., 2014. Anal. Chem. 86, 419-426.

(40) Zhao, X., Du, J., Wu, Y.Z., Liu, H.Z., Hao, X.P., 2013. J. Mater. Chem. A 1, 11748-11753.

(41) Hopt, A., Korte, S., Fink, H., Panne, U., Niessner, R., Jahn, R., Kretzschmar, H., Herms, J., 2003. J. Neurosci. Methods 128(1), 159-172.